Agostic interaction and intramolecular proton transfer from the protonation of dihydrogen ortho metalated ruthenium complexes

Andrew Toner[†], Jochen Matthes[†‡], Stephan Gründemann[‡], Hans-Heinrich Limbach[‡], Bruno Chaudret[†], Eric Clot[§], and Sylviane Sabo-Etienne[†¶]

[†]Laboratoire de Chimie de Coordination du Centre National de la Recherche Scientifique, Associé à l'Université Paul Sabatier, 205 route de Narbonne, 31077 Toulouse Cedex 04, France; [‡]Institute of Chemistry, Freie Universität Berlin, Takustrasse 3, D-14195 Berlin, Germany; and [§]Laboratoire de Structure et Dynamique des Systèmes Moléculaires et Solides (Centre National de la Recherche Scientifique, Unité Mixte de Recherche 5253), Institut Charles Gerhardt, case courrier 14, Université Montpellier II, Place Eugène Bataillon, 34000 Montpellier, France

Edited by Jay A. Labinger, California Institute of Technology, Pasadena, CA, and accepted by the Editorial Board January 17, 2007 (received for review October 13, 2006)

Protonation of the ortho-metalated ruthenium complexes $RuH(H_2)(X)(P^iPr_3)_2$ [X = 2-phenylpyridine (ph-py) (1), benzoquinoline (bq) (2)] and $RuH(CO)(ph\text{-}py)(P^iPr_3)_2$ (3) with $[H(OEt_2)_2]^+[BAr'_4]^-$ (BAr'_4 = [(3,5-$(CF_3)_2C_6H_3)_4B$]) under H_2 atmosphere yields the corresponding cationic hydrido dihydrogen ruthenium complexes $[RuH(H_2)(H\text{-}X)(P^iPr_3)_2][BAr'_4]$ [X = phenylpyridine (ph-py) (1-H); benzoquinoline (bq) (2-H)] and the carbonyl complex $[RuH(CO)(H\text{-}ph\text{-}py)(P^iPr_3)_2][BAr'_4]$ (3-H). The complexes accommodate an agostic C–H interaction characterized by NMR and in the case of 1-H by x-ray diffraction. Fluxional processes involve the hydride and dihydrogen ligands in 1-H and 2-H and the rotation of the phenyl ring displaying the agostic interaction in 1-H and 3-H. NMR studies (lineshape analysis of the temperature-dependent NMR spectra) and density functional theory calculations are used to understand these processes. Under vacuum, one equivalent of dihydrogen can be removed from 1-H and 2-H leading to the formation of the corresponding cationic ortho-metalated complexes $[Ru(H_2)(THF)(X)(P^iPr_3)_2]^+$ [X = ph-py (1-THF), bq (2-THF)]. The reaction is fully reversible. Density functional theory calculations and NMR data give information about the reversible mechanism of C–H activation in these ortho-metalated ruthenium complexes. Our study highlights the subtle interplay between key ligands such as hydrides, σ-dihydrogen, and agostic bonds, in C–H activation processes.

C–H activation | density functional theory | hydrogen transfer | NMR | sigma bonds

Catalytic transformation of alkanes and arenes via activation of an inert C–H bond is of considerable interest and remains a challenge to chemists (1–13). Since the 1980s, many information have been gathered on the stoichiometric transformations of a C–H bond at a transition metal center (14–26). Different mechanisms are operative depending on the metal, the ligand set and the nature of the media in which the reaction is performed. They differ, *inter alia*, by the way the R–H moiety interacts with the transition metal before activation. Oxidative addition proceeds from a σ complex where the C–H bond interacts as a Lewis base with the metal, whereas σ-bond metathesis does not require precoordination of the substrate. An alternative mechanism based on the properties of σ complexes is now under consideration for late transition metals. Such a σ-complex assisted metathesis mechanism (σ-CAM) allows substrate functionalization by σ-ligand substitution. It involves the interconversion of at least two σ complexes and no change in oxidation state, thanks to the intermediacy of secondary interactions (27).

The inert character of the C–H bond is reflected by its poor properties as a ligand, even though alkane complexes have been observed (28, 29). It is thus necessary to promote the interaction of one particular C–H bond to observe selective activation. A major breakthrough was proposed by Murai in 1993 with the selective insertion of an olefin into the aromatic C–H bond ortho to an activating ketone group (Eq. **1**) (30). In this system, the key intermediate is an *ortho*-metalated complex resulting from ortho C–H bond activation, thanks to chelating assistance with the donor group. Coordination of the olefin, olefin insertion into Ru–H and C–C coupling are the subsequent steps needed to close the catalytic cycle as proposed by Kakiuchi and Murai (8).

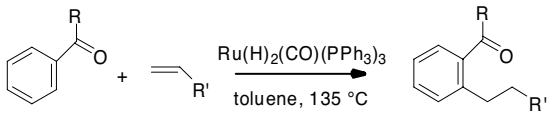

[1]

We have shown that, when using the bis-dihydrogen complex, $Ru(H)_2(H_2)_2(PCy_3)_2$, as catalyst precursor, the C–C coupling of ethylene with acetophenone or benzophenone was catalytic at room temperature (31, 32). The activity was recently improved by replacing the tricyclohexylphosphines by two tricyclopentylphosphines (33). Moreover, we were able to isolate key intermediates of general formula $RuH(H_2)(o\text{-}C_6H_5R)(PR'_3)_2$, (R = $COCH_3$, COC_6H_5) that proved to be ortho-metalated species (31). These compounds with a ketone chelating group present a very limited solubility in most of the solvents. It was thus easier to perform an in-depth study on analogous complexes, with the R substituent replaced by an aromatic N-heterocycle. In such a case, chelation is assisted by nitrogen coordination to the metal center. Indeed, we recently reported the properties of a series of ortho-metalated ruthenium hydrido complexes $Ru(H)(H_2)(X)(PiPr_3)_2$ [X = 2-phenylpyridine (ph-py), benzoquinoline (bq), phenylpyrazole (ph-pz)] resulting from C–H activation of the corresponding functionalized arene (34). These compounds display remarkable exchange couplings between the hydride and the dihydrogen ligand. Despite the nonactivity of these species toward the Murai reaction, we believed that a study focused on protonation could bring some general information, especially on the interplay between key ligands such as σ-dihydrogen or agostic bonds, as well as on hydrogen transfer processes.

Author contributions: H.-H.L., B.C., and S.S.-E. designed research; A.T., J.M., and S.G. performed research; A.T., J.M., S.G., H.-H.L., B.C., E.C., and S.S.-E. analyzed data; E.C. and S.S.-E. wrote the paper; and E.C. performed DFT calculations.

The authors declare no conflict of interest.

This article is a PNAS direct submission. J.A.L. is a guest editor invited by the Editorial Board.

Abbreviations: DFT, density functional theory; TS, transition state.

¶To whom correspondence should be addressed. E-mail: sabo@lcc-toulouse.fr.

This article contains supporting information online at www.pnas.org/cgi/content/full/0608979104/DC1.

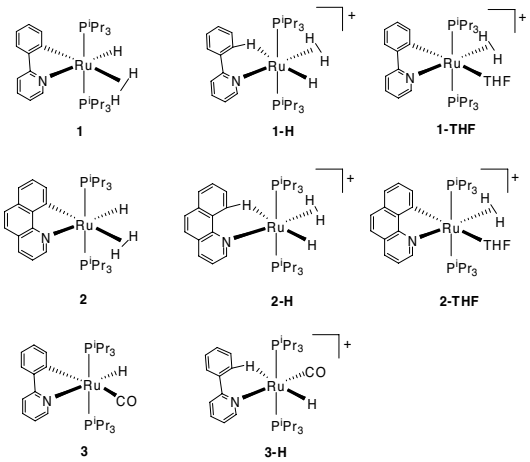

Chart 1. Structures of the ortho-metalated complexes 1–3, 1-THF, and 2-THF and the corresponding agostic complexes 1-H, 2-H, and 3-H.

The selectivity of the Murai's reaction relies on the existence of an agostic precursor, which corresponds to the very first step of the activation process of the arene substrate. We have already communicated about the characterization of such a complex, namely $[RuH(H_2)(H\text{-ph-py})(P^iPr_3)_2]^+[BAr'_4]^-$ (**1-H**), showing two coordinated σ-bonds: an agostic C–H bond and an H_2 ligand (35). **1-H** was prepared by protonation of the ortho-metalated complex $Ru(H)(H_2)(ph\text{-py})(P^iPr_3)_2$. We now report the results of a combined experimental and theoretical study on a series of agostic complexes aimed at describing their structure, the influence of the various ligands, as well as the C–H activation processes occurring within these systems. Part of this work has been communicated (35).

Results

For further details, see supporting information (SI) *Text*, Figs. 7–12, and Tables 2–6.

Synthesis and Properties of Agostic Complexes. Protonation of $RuH(H_2)(X)(P^iPr_3)_2[X = (ph\text{-py})$ (**1**), (bq) (**2**)] and $RuH(CO)(phpy)(P^iPr_3)_2$ (**3**) by $[H(OEt_2)_2]^+[BAr'_4]^-$ (BAr'_4 = [(3,5-$(CF_3)_2C_6H_3)_4B$]) at −20°C in THF, under an atmosphere of 1 bar H_2 in the case of **1** and **2**, yields the corresponding agostic cationic species $[RuH(H_2)(H\text{-ph-py})(P^iPr_3)_2]^+[BAr'_4]^-$ (**1-H**), $[RuH(H_2)(H\text{-bq})(P^iPr_3)_2]^+[BAr'_4]^-$ (**2-H**), and $[RuH(CO)(H\text{-ph-py})(P^iPr_3)_2]^+[BAr'_4]^-$ (**3-H**) (see Chart 1). Throughout the paper, we will specifically analyze the data concerning **1-H**, because it is the most interesting example (for detailed data, see *SI Text*). As previously communicated, the x-ray structure of **1-H** features two coordinated σ-bonds, agostic C–H and H–H, that are mutually *cis* (35). The ^1H NMR-spectra display in the aromatic region at room temperature broad peaks at 6.18 and 7.95 ppm for complex **1-H** (see Fig. 1). Decoalescence and sharpening of the peaks are observed when lowering the temperature. The NMR spectra below 213 K show new peaks at 4.14 and 8.22 ppm, and 7.87 and 8.30 ppm, corresponding respectively to the protons H9 and H5 on one side and H6 and H8 on the other side of the agostic phenyl ligand. The peak at 4.14 ppm was identified as H9 using an HH-COSY spectrum (see *SI Text*). The coupling between H8 and H9 is clearly observed by the cross peak at 4.14 ppm/8.30 ppm. The rate of the exchange between H5 and H9 was determined by lineshape analysis and reflects the dynamics of the phenyl ring rotation. The dependence on temperature can be expressed by the Arrhenius type equation: $k = A\ \exp(-E_a/RT)$ where k is the corresponding exchange rate, A is the frequency factor, E_a is the activation energy of the observed process, R is the ideal gas constant (8.314 J/(mol·K)), and T is the temperature (34). We found that $k = 10^{(11.3\pm0.3)}\exp((-35.6 \pm 1.8)\ kJ{\cdot}mol^{-1}/RT)\ s^{-1}$ (173 K ≤ T ≤ 303 K; k = 18,000 s^{-1} at 263 K). The value of the activation energy of the phenyl rotation process is the addition of the bond dissociation energy of the agostic interaction plus the intrinsic barrier of the phenyl ring rotation itself. The present value of E_a (35.6 kJ mol^{-1}) in complex **1-H** is low, in agreement with the weak coordination of the C–H bond. The chemical shift found for the frozen agostic proton H9 (4.14 ppm) is similar but shifted upfield compared with that observed by Crabtree and coworkers (36) in an agostic diphenylpyridine ligand (5.83 ppm). The agostic carbon was identified at 111.2 ppm for **1-H**, with a coupling constant J_{CH} of 128 Hz (THF-d_8, 183 K) as determined by a 1D-gs-HMQC experiment. The value of 128 Hz is relatively high for a C–H coupling constant of an agostic interaction that suggests a very weak activation of the C–H bond (see below) (37).

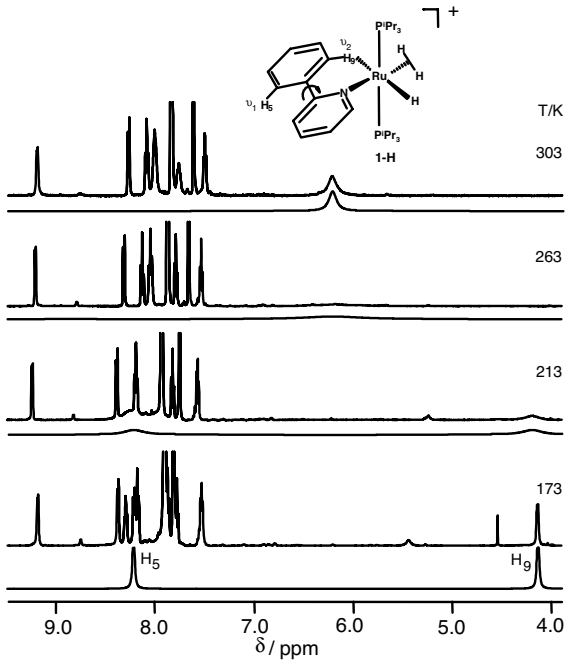

Fig. 1. Aromatic region of the experimental (top line) and simulated (bottom line) ^1H-NMR spectra (500.13 MHz) of $[RuH(H_2)(H\text{-ph-py})(P^iPr_3)_2]^+[BAr'_4]^-$ (1-H) under 800 mbar H_2 in THF-d_8. Only the exchange between *H5* and *H9* was simulated.

The hydride region in the NMR spectrum shows at room temperature one broad signal at −13.7 ppm for the hydride and the dihydrogen ligands in fast mutual exchange. Further evidence of the presence of a dihydrogen ligand was supported by T_1 measurements (T_{1min} of 16 ms at 243 K, THF-d_8, 300 MHz) and a J_{HD} value of 23 Hz obtained by deuteration of **1-H**. This J_{HD} value leads to a calculated H–H distance of 0.93 Å, whereas the T_{1min} measurement leads to a value of 0.89 Å by using a fast rotation model (38). Decoalescence is observed at low temperature, leading to a triplet at −14.12 ppm (J_{PH} = 18 Hz) for the hydride resonance and to a broad signal at −13.02 ppm for the dihydrogen ligand. The Arrhenius parameters for this process have been determined by lineshape analysis (see *SI Text*).

The activation energy of the classical hydride dihydrogen exchange in complexes **1-H** and **2-H** (47 kJ mol^{-1}) is similar to those found for complexes **1** and **2** (40.0 and 42.3 kJ mol^{-1}, respectively) (34). The ligands and the charge have little effect on the observed classical exchange processes. The spectra of complexes **1-H** and **2-H** do not present temperature-dependent quantum-mechanical exchange couplings as were displayed by complexes **1** and **2**. The nonclassical hydride dihydrogen exchange process might be too fast

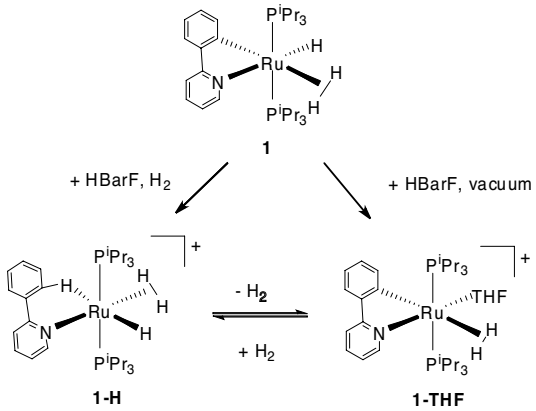

Scheme 1. Protonation in THF of $RuH(H_2)(ph\text{-}py)(P^iPr_3)_2$ (1).

to be observed by liquid state NMR spectroscopy in **1-H** and **2-H**. Due to a reduced electron density on the positively charged complexes, the dihydrogen exchange barrier might be very low and therefore the quantum mechanical exchange fast ($>10^4$ Hz) to be observed by liquid-state NMR spectroscopy (39).

We have previously described that the dihydrogen ligand in **1** can easily be substituted by N_2, O_2, or C_2H_4 (34). In the context of the Murai reaction, it was interesting to test the protonation of the ethylene complex $RuH(C_2H_4)(ph\text{-}py)(P^iPr_3)_2$ (**4**). Because **4** loses immediately ethylene in solution, the protonation with $[H(OEt_2)_2]^+[BAr'_4]^-$ was performed under an atmosphere of 800 mbar ethylene in THF-d_8. When the reaction was carried out below room temperature, a new complex, $[Ru(H_2)(THF)(ph\text{-}py)(P^iPr_3)_2]^+$ (**1-THF**), was formed exclusively (see below and Chart 1). At higher temperatures, a mixture of products was observed and formation of ethane was detected.

Proton Transfer Reactions. **1-H** and **2-H** are not stable in solution. They transform into new orthometalated complexes $[Ru(H_2)(THF)(X)(P^iPr_3)_2]^+$ [X = ph-py (**1-THF**), bq (**2-THF**)] if H_2 is removed from the THF solution by pumping or upon heating to 65°C in a THF-d_8 solution inside an NMR tube (see Chart 1 and Scheme 1). THF adducts could not be isolated but their properties were studied by NMR spectroscopy and density functional theory (DFT) calculations (see below). All of the data support the preferred geometry shown in Scheme 1. The NMR data obtained for **1-THF** are in agreement with the presence of a single dihydrogen molecule and the absence of any hydride or agostic proton in the coordination sphere of the metal. A broad signal was observed at −7.53 ppm which displays a short T_{1min} value of 11 ms at 263 K and 300 MHz. Upon deuteration, the hydride signal transforms into a 1:1:1 triplet (J_{HD} = 27 Hz) in agreement with the presence of an unstretched dihydrogen ligand. Moreover, the presence of a metalated carbon is inferred from the resonance at 169 ppm in the $^{13}C\{^1H\}$ NMR spectrum. The reaction can be reversed when a solution of **1-THF** is placed under H_2. Therefore, this reaction represents an easy and reversible C–H activation process at room temperature. It is worth noting that a similar process was reported by Crabtree and coworkers (36) for an iridium complex with a diarylpyridine ligand and by Milstein and coworkers (40–42) for a rhodium complex with an aryl phosphane ligand. It is interesting that, upon placing **1-H** in a deuterium atmosphere, exclusive deuteration of the ortho positions of the phenyl ring is observed, demonstrating the presence of an equilibrium between **1-H** and a metalated intermediate.

Computational Studies

Structure of the Agostic Complexes. To gain further insight into the structure and the dynamic properties of the agostic complexes, model systems $[Ru(H)(H\text{-}ph\text{-}py)(L)(PMe_3)_2]^+$ (L = H_2, **1q-H**; L = CO, **3q-H**; L = C_2H_4, **4q-H**; L = vacant site, **5q-H**) were optimized at the B3PW91 level. In all these complexes, the agostic C–H bond is *trans* to the hydride ligand as was the case in the structure of **1-H**.[35] The optimized geometry for **1q-H** is in excellent agreement with the experimental data. The agostic Ru···C bond distance [2.528(3) Å, **1-H**; 2.513 Å, **1q-H**] and the dihedral angle between the two rings [27.5(4)°, **1-H**; 24.1°, **1q-H**] are particularly well reproduced. The agostic C–H bond is only slightly elongated in comparison to the other aromatic C–H bonds within the phenyl ring (1.123 Å, **1q-H**), as a result of the weak interaction with the metal center. The DFT calculations confirm the presence of an H_2 ligand *trans* to N. The H–H bond distance is longer than in **1-H** [0.82(4) Å, **1-H**; 0.946 Å, **1q-H**] but compares well with the value deriving from NMR data (0.93 Å, J_{HD}; 0.89 Å, T_{1min}).

In the case of **3-H,** and in the absence of any x-ray data, it was difficult to ascertain the geometry of the ligands around the ruthenium center. As formation of an agostic interaction and subsequent activation of the C–H bond are critically influenced by the respective nature of the ligand *cis* and *trans* to the agostic bond, DFT calculations have been performed on $[Ru(H)(H\text{-}ph\text{-}py)(CO)(PMe_3)_2]^+$ with the hydride *trans* (**3q-H**) and *cis* (**3qcis-H**) to the agostic bond. Even though the corresponding experimental systems were not characterized, the calculations were also carried out on the two isomers of $[Ru(H)(H\text{-}ph\text{-}py)(C_2H_4)(PMe_3)_2]^+$ (**4q-H** and **4qcis-H**) and $[Ru(H)(H\text{-}ph\text{-}py)(PMe_3)_2]^+$ (**5q-H** and **5qcis-H**). A structure corresponding to **1qcis-H** could not be found as a local minimum, and the optimization procedure yielded **1q-H** for different starting geometries featuring an H_2 ligand *trans* to the agostic bond. The DFT calculations indicate that the isomers with the hydride *trans* to the agostic bond are more stable than the other isomers (Table 1). The energy difference of 25.1 kJ mol^{-1} between **3q-H** and **3qcis-H** is large enough to set **3q-H** as a model for **3-H**. This finding is in agreement with the preferred structure proposed from the NMR studies. Selected geometrical parameters pertinent to the agostic interaction are given in Table 1. For the carbonyl and ethylene species, the relative energies of the two isomers are similar.

In this context, NMR measurements are particularly suited to investigate agostic interactions. Low temperature experiments allow access to useful information on the dynamic of the system

Table 1. Selected bond distances (Å) for the agostic interaction, calculated chemical shift δ_H (ppm) of the agostic proton, calculated coupling constant J_{CH} (Hz), relative energy ΔE (kJ mol^{-1}), and activation energy $\Delta E^{\#}$(Ph) (kJ mol^{-1}) for the phenyl-ring rotation for the calculated agostic species $[Ru(H)(H\text{-}ph\text{-}py)(L)(PMe_3)_2]^+$

	1q-H, L = H_2	3q-H, L = CO	3qcis-H, L = CO	4q-H, L = C_2H_4	4qcis-H, L = C_2H_4	5q-H, no L	5qcis-H, no L
C–H	1.123	1.119	1.112	1.122	1.134	1.125	1.277
Ru·C	2.513	2.553	2.568	2.548	2.445	2.506	2.120
Ru·H	1.918	1.954	1.980	1.913	1.839	1.908	1.620
δ_H	4.6	4.2	3.2	4.9	2.7	6.7	−21.9
J_{CH}	120.6	122.6	120.0	121.5	112.3	121.0	78.7
ΔE	—	0.0	25.1	0.0	23.7	0.0	35.9
$\Delta E^{\#}$(Ph)	35.0	30.4	35.9	29.5	51.8	35.8	83.3

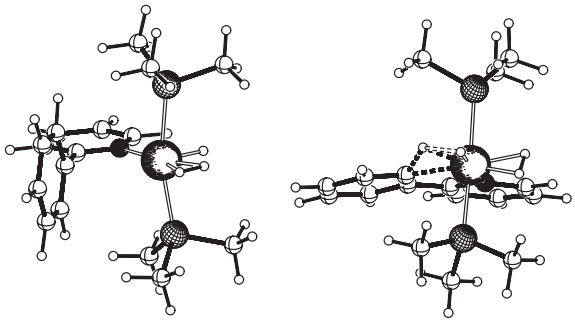

Fig. 2. B3PW91 optimized TS geometries. (*Left*) 1q-H^{TSROT} for phenyl-ring rotation within the agostic complex 1q-H. (*Right*) 1q-H^{TSTR}, for H-transfer from the agostic complex 1q-H.

(chemical shifts), and the magnitude of the agostic interaction can be monitored by J_{CH} values. NMR calculations of the chemical shift of the agostic proton and of the J_{CH} coupling constant were carried out with the hybrid PBE1PBE functional and IGLOO-II basis sets (see *SI Text*). In the case of **1-H**, low temperature NMR data yielded an agostic interaction characterized by a chemical shift of 4.14 ppm and a J_{CH} coupling constant of 128 Hz. The calculated values of 4.6 ppm and 120.6 Hz for **1q-H** compare well with the experimental values. In the case of **3-H**, the low temperature NMR data yielded a proton chemical shift of 4.31 ppm and a J_{CH} coupling constant of 130 Hz for the agostic bond. The calculated values of 4.2 ppm and 122.6 Hz for **3q-H** are also in better agreement with experimental NMR data than those of **3qcis-H** (3.2 ppm and 120 Hz).

Phenyl Ring Rotation. As shown above, we have evidenced by NMR an exchange process of the H5, H9 protons due to phenyl ring rotation. We have located, on the potential energy surface, a transition state (TS) for the phenyl ring rotation, **1q-H^{TSROT}** (Fig. 2), at 35.0 kJ mol^{-1} above **1q-H** (Table 1). In **1q-H^{TSROT}**, the phenyl ring is perpendicular to the pyridine ring (dihedral angle 92.7°), and the C–H bond, which was agostic in **1q-H** (1.123 Å), now presents a normal value (1.086 Å). The agostic interaction has thus disappeared in the TS. This finding is confirmed by the shortening of the Ru-H distance *trans* to the agostic (1.571 Å, **1q-H**; 1.547 Å, **1q-H^{TSROT}**). The Ru-N bond also shortens in **1q-H^{TSROT}** (2.123 Å, **1q-H**; 2.101 Å, **1q-H^{TSROT}**) as a result of the relief of strain in the agostic interaction. The H–H distance in the H_2 ligand remains unchanged (0.94 Å). The calculated value for the activation barrier associated to phenyl ring rotation (35.0 kJ mol^{-1}) is in excellent agreement with the experimental value obtained for ortho-H exchange in **1-H** (35.6 kJ mol^{-1}). The calculations thus support phenyl ring rotation as the origin of the observed H-site exchange process.

The calculated activation barrier of 30.4 kJ mol^{-1} for **3q-H^{TSROT}**, is not in such a good agreement with the experimental value (44.5 kJ mol^{-1}, for **3-H**). To gain further insight in the properties of these systems, calculations were also carried out on complexes not experimentally observed. The transition state for phenyl ring rotation of all of the agostic complexes were optimized (Table 1). They exhibit similar geometrical features with perpendicular phenyl and pyridine rings. When a hydride ligand is *trans* to the agostic bond, the activation barrier for phenyl ring rotation is rather insensitive to the actual nature of the ligand *cis* to the agostic bond (see **1q-H**, **3q-H**, **4q-H**, and **5q-H** in Table 1). When the hydride ligand is *cis* to the agostic bond, the activation barrier experiences larger variation depending on the nature of the *trans* ligand. Absence of the latter drastically increases the activation barrier (83.3 kJ mol^{-1}, **5qcis-H**), and the reduction of the activation barrier correlates with the π-accepting properties of the ligand (51.8 kJ mol^{-1} for L = C_2H_4; 35.9 kJ mol^{-1} for L = CO); the more π-acid the ligand *trans* to the agostic, the easier the rotation. It is interesting to note that, in **4qcis-H**, the C_2H_4 ligand lies in the equatorial plane defined by Ru, pyridine, and hydride. Therefore, the agostic bond is not competing for the same t_{2g} orbital in the back-donation interactions. The situation is different with CO in **3qcis-H** as the latter possesses two π-accepting MOs, and there is thus competition with the C–H agostic bond for the same t_{2g} orbital. This competition weakens the agostic interaction as illustrated by both the geometrical parameters and the values of the activation barrier for phenyl ring rotation.

Proton Transfer Studies. The complex **1-H**, featuring two coordinated σ-bonds in *cis* position, is not stable in solution and transforms into an orthometalated complex **1-THF** stabilized by solvent (THF) coordination (Scheme 1). We first examined the hydrogen transfer from **1q-H** (the model for **1-H**), to **1q-H$_2$** (the model for **1-THF**) but replacing THF by H_2 (see Scheme 2). The transition state, **1q-H^{TSTR}**, for the hydrogen transfer from the agostic carbon to Ru has been located on the potential energy surface and lies 75.4 kJ mol^{-1} above **1q-H** (Fig. 2). The transition state connects to the *bis*–dihydrogen complex **1q-H$_2$** at 8.2 kJ mol^{-1} above **1q-H**. The Ru-C bond is almost formed in the TS (2.152 Å) and one hydrogen atom of the H_2 ligand that was *cis* to the agostic bond in **1q-H**, has been transferred to the hydride ligand *trans* to the forming Ru-C bond to accommodate the change in nature of the ligand from weak (agostic) to strong (aryl). This new H–H interaction in **1q-H^{TSTR}** is typical of an H_2 ligand (0.862 Å). As a consequence, there is now a basic site (the hydride) *cis* to the transferring H and the H···H distance of 1.711 Å is typical of a dihydrogen bond but the transferring H is also close to Ru (1.56 Å). The TS in **1q-H^{TSTR}** could thus be described as a Ru^{IV} dihydride dihydrogen complex. Whatever the nature of the TS, the final product is a Ru^{II} *bis*–dihydrogen complex and no Ru^{IV} intermediate could be located on the PES.

The *bis*–dihydrogen complex **1q-H$_2$** presents two potential labile ligands and, upon substitution of one H_2 ligand by Me_2O (as a model for THF), two different complexes were optimized. The isomer with Me_2O *cis* to the phenyl ring, **1qcis-Me$_2$O**, lies at 45.0 kJ mol^{-1} above **1q-H**, whereas the other isomer with Me_2O *trans* to the phenyl ring, **1q-Me$_2$O**, lies at 25.0 kJ mol^{-1} above **1q-H** (Scheme 2). Substitution of the H_2 ligand *trans* to the strongest σ-donor ligand (aryl) is clearly favored. The complex **1q-Me$_2$O** is 16.8 kJ mol^{-1} less stable than the *bis*–dihydrogen complex **1q-H$_2$**, yet the experimental observations point to the formation of an orthometallated complex with only one coordinated H_2 molecule. It should be noted

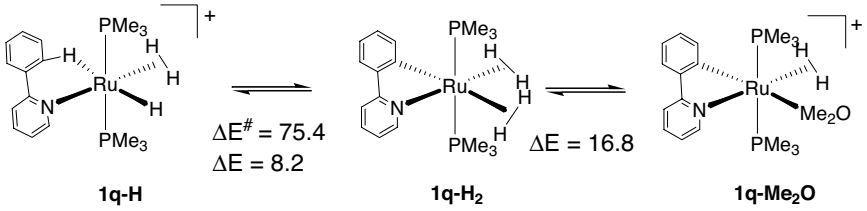

Scheme 2. Proton transfer from the agostic species 1q-H to the orthometalated species 1q-H_2 and 1q-Me_2O (energies in kJ mol^{-1}).

that **1-THF** was obtained when H_2 was removed from the THF solution by pumping or upon heating at 65°C. Heating is needed to overcome the activation barrier for proton transfer. In solution with a good coordinating solvent such as THF, we may assume that the more labile H_2, *trans* to the aryl, dissociates and is replaced by a solvent molecule. It is interesting to note that the two complexes, **1q-H** and **1q-H$_2$**, are very close in energy, in agreement with the reversibility of the reactions observed experimentally. The labeling experiments also support the proposed mechanism. Reaction of **1-H** with D_2 leads to exclusive deuteration of the ortho positions of the phenyl ring in agreement with an equilibrium between **1-H** and a *bis*–dihydrogen metalated intermediate analogous to the model **1q-H$_2$**. A succession of H(D)-transfer reactions, coupled with phenyl ring rotation will eventually incorporate deuterium exclusively at the ortho-positions.

Discussion

The Agostic Interaction. Formation of an agostic interaction of the C–H bond ortho to the activating group is a key step in the Murai's reaction. The complexes **1-H, 2-H**, and **3-H** present such an interaction, and NMR studies highlighted various aspects of the interaction. The strength of any agostic interaction is generally inferred from the reduction of the J_{CH} coupling constant and the high field shift of the proton resonance. In the present case, both indicators are very close. The calculated trend for the J_{CH} coupling constant is faithfully reproduced but the proton chemical shift for **3q-H** (4.2 ppm) is calculated lower than **1q-H** (4.6 ppm) contrary to experiment. However, proton chemical shifts are difficult to compute accurately, particularly when interaction with a metal is present.

It is always difficult to estimate the intrinsic strength of an agostic interaction because definition of a strictly agostic-free configuration is not obvious. In our complexes, the energy of the H-site exchange process of the ortho hydrogen atoms was evaluated from NMR studies at variable temperature. The exchange was shown to proceed along a TS featuring a phenyl ring perpendicular to the pyridine ring (Fig. 2). In such a configuration the C–H ortho bonds are clearly not agostic. The activation barrier could thus serve to estimate the strength of the agostic interaction in **1-H** and **3-H**. However, the phenyl-pyridine ligand possesses an intrinsic rotation barrier which was estimated to be 19.6 kJ mol^{-1} from DFT(B3PW91) calculations. This allows the estimation of the strength of the agostic interaction in **1-H** and **3-H**, namely 16 kJ mol^{-1} and 24.9 kJ mol^{-1}, respectively. As expected, these agostic interactions are weak in nature, and the calculated values compare well with the experimental data of 41.8 ± 25 kJ mol^{-1} obtained for intramolecular W···H—C agostic interactions in $W(CO)_3(PCy_3)_2$ by Hoff and coworkers (43). The above results point to a slightly stronger interaction in **3-H** than in **1-H**, contrary to what has been inferred from the proton chemical shift and J_{CH} coupling constant values; this illustrates the difficulty to obtain quantitative information on such weak interactions.

To gain further insight, calculations on systems not observed experimentally were carried out. In these complexes, an agostic interaction is always present but the nature of the ligands *cis* and *trans* to the agostic bond is varied. The value of the activation barrier for phenyl-ring rotation can be used as an indicator of the strength of the agostic interaction. From the results in Table 1, for a given ligand *trans* to the agostic (i.e., hydride), changing the nature of the *cis* ligand does not drastically alter the general features of the agostic interaction (see **1q-H**, **3q-H**, **4q-H**, and **5q-H**). The C–H bond distances have very similar values (≈1.12 Å), and the J_{CH} coupling constants have values lying within 2 Hz. Also, the activation barriers for phenyl-ring rotation are very close with the lowest value (29.5 kJ mol^{-1}, **4q-H**), only 6.3 kJ mol^{-1} smaller than the highest one (35.8 kJ mol^{-1}, **5q-H**).

When the ligand in *trans* is varied, while keeping the same ligand in *cis* (i.e., hydride), the agostic interaction experiences larger variation. In the extreme case of **5qcis-H**, where no *trans* ligand is present, strong C–H activation is observed. The C–H bond is strongly elongated and the Ru-C bond is formed (Table 1). The proton chemical shift (−21.9 ppm) is also in agreement with a strong Ru···H interaction. The complex could be considered as a Ru^{IV} dihydride. The relative energy between the two isomers (35.9 kJ mol^{-1}) is in agreement with the description of **5qcis-H** as a Ru^{IV} complex lying at higher energy than the Ru^{II} isomer **5q-H**. With a strong σ-donor and π-acceptor such as CO (**3qcis-H**) the situation is not very different from that for the pure σ-donor H (**3q-H**). Changing the *trans* ligand for a weaker σ-donor, such as C_2H_4 (**4qcis-H**), strengthens the agostic interaction. In particular, the J_{CH} coupling constant is significantly reduced (112.5 Hz) and the activation barrier for phenyl-ring rotation is substantially larger (51.8 kJ mol^{-1}). All of the above results point to a critical influence of the σ-donor properties of the ligand *trans* to the agostic bond to tune this interaction.

The agostic interaction is generally described as the result of two synergistic electron transfers: σ-donation from the C–H bond to the metal and π back-donation from the metal in the σ^*(C–H) orbital. Within the natural bonding orbital (NBO) scheme, these two contributions have been evaluated with the second-order donor–acceptor perturbation procedure of NBO (44). These energetic stabilizations reflect the magnitude, not in an absolute way, of the electron transfer. As a result of these hyperconjugative interactions, the natural localized molecular orbital (NLMO) of the σ(C–H) agostic bond does contain some Ru character and the extent of the hyperconjugative interaction is reflected by the weight of the parent NBO in the NLMO. Stronger delocalization is associated to lower NBO weight. The results clearly show that donation from the σ(C–H) bond toward the σ^*(Ru-L$_t$) antibond (between Ru and the ligand L$_t$ *trans* to the agostic bond) is the major contribution to the agostic interaction. For the systems with the hydride *trans* to the agostic, the characteristics of the agostic interaction are very similar. The actual nature of the *cis* ligand only slightly modifies the electronic impact of the *trans* ligand on the strength of the agostic. For **3qcis-H**, switching the role of H and CO does not lead to a significant alteration of the agostic interaction as the σ-donor properties of H and CO are very similar. It clearly illustrates that the π-accepting properties of the *trans* ligand have no strong influence on the agostic bond. The major difference observed in **4qcis-H** is the large increase in the σ-donation contribution from σ(C–H). This allows significant hyperconjugative delocalization as illustrated by the Ru-content of the NLMO (4.9%) and by the lower weight of the parent NBO in the NLMO (90.9%). There is thus clearly a stronger agostic interaction in **4qcis-H** originating from the lower σ-donor character of the ethylene ligand *trans* to the agostic bond.

Proton Transfer Reactions. In the Murai's system, after coordination of the ortho C–H bond, C–H activation is necessary to obtain an ortho-metalated complex as an intermediate before the C–C coupling step. To design more efficient catalysts, it is thus desirable to better understand the factors influencing this C–H bond breaking step. To test the influence of the presence of a *cis* hydride on the hydrogen transfer, the two TS, **5qcis-H^{TSTR}** and **5q-H^{TSTR}**, originating from the agostic complexes with one vacant site remaining in the coordination sphere of the metal, **5qcis-H** and **5q-H**, respectively, have been optimized. The most striking differences between the two systems lie in the values of the activation barriers: 0.5 kJ mol^{-1} for **5qcis-H^{TSTR}** and 122.8 kJ mol^{-1} for **5q-H^{TSTR}**. From the geometrical parameters, both TS could be described as Ru^{IV} complexes (agostic C–H bond broken and formation of strong Ru-H and Ru-C bonds), but the difference in activation barrier is difficult to explain. One may argue that the absence of a ligand *trans* to the forming Ru–C bond in **5qcis-H^{TSTR}**, whereas a strong σ-donor is present in **5q-H^{TSTR}**, is the reason for the easier C–H activation in the former. As a matter of fact, the activation barrier for **1q-H^{TSTR}** is 75.4 kJ mol^{-1} with an H_2 ligand *trans* to Ru–C.

To further test the influence of the nature of the ligand *trans* to the agostic bond in the proton transfer, the TS with Me_2O *trans* to the agostic, **6qcis–Me$_2$O^{TSTR}**, has been optimized. The activation barrier is only 6.4 kJ mol^{-1}, thus showing the critical influence of the nature of the *trans* ligand. The agostic complex **6qcis–Me$_2$O**, before proton transfer, exhibits a very strong agostic interaction as inferred from the C–H bond distance (1.200 Å) and the calculated J_{CH} coupling constant (91.3 Hz). These results indicate that there is a good correlation between the strength of the agostic interaction and the activation of that bond. A strong agostic interaction correlates with an easy C–H activation process.

Complexes **1-H** and **2-H** exhibit reactivity patterns in agreement with reversible C–H bond breaking and bond making processes. The calculations have located the TS for H-transfer in **1q-H** (Fig. 2) and the main features of this TS is the reorganization of the hydrides in the coordination sphere of the metal. Concomitant to the C–H breaking process, there is a transfer of one hydrogen of the H_2 ligand that was *cis* to the agostic in **1q-H** to the hydride *trans* to the agostic. In **1q-H^{TSTR}**, there is now an optimal organization of the weak and strong ligands to accommodate both the formation of Ru-C (*trans* to H_2) and the transfer of H as a proton to the basic nearby hydride (*trans* to N). The geometrical features of this TS could be interpreted in two different ways. The short Ru-H distances for the transferring H and the *cis* hydride (1.56 and 1.60 Å, respectively), together with the already formed Ru-C bond (2.152 Å) could allow the description of **1q-H^{TSTR}** as a Ru^{IV} dihydrogen–dihydride complex. The product of the transfer being a *bis*–dihydrogen Ru^{II} complex, this process would be akin to the oxidative addition hydrogen transfer mechanism as described by Goddard and coworkers (45) in the case of hydroarylation catalysts. Another alternative, as the H···H distance between the transferring H and the *cis* hydride is 1.711 Å, is the formation of a very stretched H_2 ligand in the TS, or at least of a dihydrogen bonded stabilized H-transfer. This would correspond to a Ru^{II} *bis*–dihydrogen TS and the transfer could be described as a prototype of a σ-CAM mechanism, as described by Perutz and Sabo-Etienne (27).

In summary, we have examined the protonation of a series of ortho-metalated Ru complexes by combining NMR and DFT studies. These complexes can serve as models for one of the key species in the Murai reaction. Our findings on the resulting agostic complexes indicate a critical influence of the σ-donor properties of the ligand *trans* to the agostic bond to tune this interaction and give rise to subsequent C–H activation. We hope that further studies will enable us to develop new catalysts with reasonably strong agostic bonds that promote easier C–H activation processes.

Materials and Methods

All reactions were carried out under argon by using Schlenk glassware and vacuum line or glove box techniques. Complexes $RuH(H_2)(X)(P^iPr_3)_2$ [X = 2-phenylpyridine (ph-py) (**1**), benzoquinoline (bq) (**2**)], and RuH(CO)(ph-py)(P^iPr_3)$_2$ (**3**) were prepared according to the procedures described in ref. 34. $[H(OEt_2)_2]^+[BAr'_4]^-$ (BAr'_4 = [(3,5-$(CF_3)_2C_6H_3)_4B$]) was prepared according to ref. 46. See *SI Text* for **2-H**, **3H**, and **2-THF.** All of the calculations have been performed with the Gaussian03 package, at the B3PW91 level; see *SI Text* for more details.

[RuH(H$_2$)(H-ph-py)(P^{i}Pr$_3$)$_2$]$^+$[Bar′4]$^-$ (1-H). A Fisher-Porter bottle was loaded with $RuH(H_2)(ph\text{-}py)(P^iPr_3)_2$ (**1**) (0.46 g, 0.49 mmol) and $[H(OEt_2)_2]^+[BAr'_4]^-$ (0.79 g, 0.79 mmol) and cooled to −78°C. After ≈10 min, 15 ml of THF was added, yielding a pale orange solution whereby the solids remained essentially insoluble at this temperature. The bottle was then immersed in liquid nitrogen and the heterogeneous mixture thoroughly degassed during three freeze and thaw cycles. The bottle was then pressurized with H_2 (3 bar) at −78°C. Warming to room temperature over a period of ≈45 min, led to the formation of an orange solution; no gas evolution was observed during the reaction even at room temperature. Subsequently, the solution was pressurized with H_2 (3 bar). Orange crystals of **1-H**, suitable for x-ray diffraction analysis, were obtained at room temperature under H_2 (0.54 g, 70%). The compound is best stored under an atmosphere of H_2 at −20°C; it rapidly decomposes in the solid state *in vacuo*. See *SI Text* for NMR data.

[Ru(H$_2$)(ph-py)(THF)(P^{i}Pr$_3$)$_2$]$^+$[Bar′$_4$]$^-$ (1-THF). Complex **1** (20 mg) was mixed with 35 mg $[H(OEt_2)_2]^+[BAr'_4]^-$ in a NMR-tube inside a glove-box. THF (1.5 ml) was condensed into the tube and slowly warmed up to room temperature. Significant gas evolution was observed (degassing from time to time ensured that no overpressure was in the tube). Complete protonation was achieved by using an ultrasonic bath until total dissolution and no more gas evolution (≈5 min). THF was evaporated, and the solid was washed three times with 1 ml of pentane. The resulting solid was dried for 1 h at 10^{-6} torr. After this time, 1 ml of THF-d_8 was condensed on the solid, and the sample was flame sealed. See *SI Text* for NMR data.

This work was supported by the Deutsche Forschungsgemeinschaft (Bonn, Germany), the Fonds der Chemischen Industrie, the University Montpellier 2, and the Centre National de la Recherche Scientifique. We also thank the European Union through the Human Capital Mobility program, Hydrogen Localization and Transfer network.

1. Sen A (1998) *Acc Chem Res* 31:550–557.
2. Guari Y, Sabo-Etienne S, Chaudret B (1999) *Eur J Inorg Chem* 7:1047–1055.
3. Kakiuchi F, Murai S (1999) *Topics in Organometallic Chem* 3:47–79.
4. Dyker G (1999) *Angew Chem Int Ed* 38:1699–1712.
5. Jia C, Kitamura T, Fujiwara Y (2001) *Acc Chem Res* 34:633–639.
6. Trost BM, Toste FD, Pinkerton AB (2001) *Chem Rev* 101:2067–2096.
7. Ritleng V, Sirlin C, Pfeffer M (2002) *Chem Rev* 102:1731–1769.
8. Kakiuchi F, Murai S (2002) *Acc Chem Res* 35:826–834.
9. Kakiuchi F, Chatani N (2003) *Adv Synth Catal* 345:1077–1101.
10. Kubas GJ (2005) *Catal Lett* 104:79–101.
11. Ishiyama T, Miyaura N (2003) *J Organomet Chem* 680:3–11.
12. Goldman AS, Goldberg KI (2004) *ACS Symp Ser* 885:1–43.
13. Hartwig JF, Cook KS, Hapke M, Incarvito CD, Fan Y, Webster CE, Hall MB (2005) *J Am Chem Soc* 127:2538–2552.
14. Crabtree RH (1985) *Chem Rev* 85:245–269.
15. Jones WD, Feher FJ (1989) *Acc Chem Res* 22:91–100.
16. Arndtsen BA, Bergman RG, Mobley TA, Peterson TH (1995) *Acc Chem Res* 28:154–162.
17. Shilov AE, Shul'pin GB (1997) *Chem Rev* 97:2879–2932.
18. Stahl SS, Labinger JA, Bercaw JE (1998) *Angew Chem Int Ed* 37:2181–2192.
19. Jones WD (1999) *Topics Organometallic Chem* 3:9–46.
20. Crabtree RH (2001) *J Chem Soc Dalton Trans* 24372450. 2437–2450.
21. Labinger JA, Bercaw JE (2002) *Nature* 417:507–514.
22. Jones WD (2005) *Inorg Chem* 44:4475–4484.
23. Crabtree RH (2004) *J Organomet Chem* 689:4083–4091.
24. Lersch M, Tilset M (2005) *Chem Rev* 105:2471–2526.
25. Owen JS, Labinger JA, Bercaw JE (2006) *J Am Chem Soc* 128:2005–2016.
26. Feller M, Karton A, Leitus G, Martin JML, Milstein D (2006) *J Am Chem Soc* 128:12400–12401.
27. Perutz RN, Sabo-Etienne S (2007) *Angew Chem Int Ed*, in press.
28. Hall C, Perutz RN (1996) *Chem Rev* 96:3125–3146.
29. Lawes DJ, Geftakis S, Ball GE (2005) *J Am Chem Soc* 127:4134–4135.
30. Murai S, Kakiuchi F, Sekine S, Tanaka Y, Kamatani A, Sonoda M, Chatani N (1993) *Nature* 366:529–531.
31. Guari Y, Sabo-Etienne S, Chaudret B (1998) *J Am Chem Soc* 120:4228–4229.
32. Guari Y, Castellanos A, Sabo-Etienne S, Chaudret B (2004) *J Mol Cata A* 212:77–82.
33. Grellier, M. Vendier L, Chaudret B, Albinati A, Rizzato S, Mason SA, Sabo-Etienne S (2005) *J Am Chem Soc* 127:17592–17593.
34. Matthes J, Gründemann S, Toner A, Guari Y, Donnadieu B, Spandl J, Sabo-Etienne S, Clot E, Limbach H–H, Chaudret B (2004) *Organometallics* 23:1424–1433.
35. Toner AJ, Gründemann S, Clot E, Limbach H-H, Donnadieu B, Sabo-Etienne S, Chaudret B (2000) *J Am Chem Soc* 122:6777–6778.
36. Albeniz AC, Schulte G, Crabtree RH (1992) *Organometallics* 11:242–249.
37. Brookhart M, Green MLH, Wong LL (1988) *Prog Inorg Chem* 36:1–124.
38. Kubas GJ (2001) *Metal Dihydrogen and s-Bond Complexes* (Kluwer Academic/Plenum, New York).
39. Sabo-Etienne S, Chaudret B (1998) *Chem Rev* 98:2077–2091.
40. Vigalok A, Uzan O, Shimon LJW, Ben-David Y, Martin JML, Milstein D (1998) *J Am Chem Soc* 120:12539–12544.
41. Rybtchinski B, Konstantinovsky L, Shimon LJW, Vigalok A, Milstein D (2000) *Chem Eur J* 6:3287–3292.
42. Rybtchinski B, Cohen R, Ben-David Y, Martin JML, Milstein D (2003) *J Am Chem Soc* 125:11041–11050.
43. Gonzalez AA, Zhang K, Nolan SP, Lopez de la Vega R, Mukerjee SL, Hoff CD, Kubas GJ (1988) *Organometallics* 7:2429–2435.
44. Reed AE, Curtiss LA, Weinhold F (1988) *Chem Rev* 88:899–926.
45. Oxgaard J, Periana RA, Goddard WA, III (2004) *J Am Chem Soc* 126:11658–11665.
46. Brookhart M, Grant B, Volpe AF, JR (1992) *Organometallics* 11:3920–3922.